Biogeosciences Discuss., 12, 20149–20178, 2015
www.biogeosciences-discuss.net/12/20149/2015/
doi:10.5194/bgd-12-20149-2015


Biogeosciences Discussions
Open Access



# High resolution wetland mapping in West Siberian taiga zone for methane emission inventory

**I. E. Terentieva[1,*], M. V. Glagolev[1,2,3], E. D. Lapshina[2], A. F. Sabrekov[1], and S. S. Maksyutov[4]**

[1]Tomsk State University, Tomsk, Russia
[2]Yugra State University, Khanty-Mansyisk, Russia
[3]Moscow State University, Moscow, Russia
[4]National Institute for Environmental Studies, Tsukuba, Japan
[*]previously published as I. E. Kleptsova

Received: 5 November 2015 – Accepted: 25 November 2015 – Published: 16 December 2015

Correspondence to: I. E. Terentieva (kleptsova@gmail.com)

Published by Copernicus Publications on behalf of the European Geosciences Union.

## Abstract

High latitude wetlands are important for understanding climate change risks because these environments sink carbon and emit methane. Fine scale heterogeneity of wetland landscapes pose challenges for producing the greenhouse gas flux inventories based on point observations. To reduce uncertainties at the regional scale, we mapped wetlands and water bodies in the taiga zone of West Siberia on a scene-by-scene basis using a supervised classification of Landsat imagery. The training dataset was based on high-resolution images and field data that were collected at 28 test areas. Classification scheme was aimed at methane inventory applications and included 7 wetland ecosystem types composing 9 wetland complexes in different proportions. Accuracy assessment based on 1082 validation polygons of 10 × 10 pixels indicated an overall map accuracy of 79 %. The total area of the wetlands and water bodies was estimated to be 52.4 Mha or 4–12 % of the global wetland area. Ridge-hollow complexes prevail in WS's taiga, occupying 33 % of the domain, followed by forested bogs or "ryams" (23 %), ridge-hollow-lake complexes (16 %), open fens (8 %), palsa complexes (7 %), open bogs (5 %), patterned fens (4 %), and swamps (4 %). Various oligotrophic environments are dominant among the wetland ecosystems, while fens cover only 14 % of the area. Because of the significant update in the wetland ecosystem coverage, a considerable revaluation of the total $CH_4$ emissions from the entire region is expected. A new Landsat-based map of WS's taiga wetlands provides a benchmark for validation of coarse-resolution global land cover products and wetland datasets in high latitudes.

## 1 Introduction

High latitude wetlands are important for understanding climate change mechanism as they provide long term storage of carbon and emit significant amount of methane. West Siberia (WS) is the world's largest high-latitude wetland system situating in the high latitudes experiencing accelerated rate of climate change (Solomon et al., 2007).

It was found both at global and regional scales that poorly constrained estimates of wetland and lake area is a major uncertainty in predicting current and future of greenhouse gas budget (Melton et al., 2013; Turetsky et al., 2014; Petrescu et al., 2010). Fine scale heterogeneity of WS wetland landscapes (Bohn et al., 2007; Eppinga et al., 2010; Bridgham et al., 2013) pose challenges for producing inventories of methane emissions (Glagolev et al., 2011) and wetland net primary production (Peregon et al., 2008) which are based on large number of point scale field measurements.

Present land cover products failed to capture the fine-scale spatial variability within wetlands because mixed pixels greatly decrease the accuracy of these products. Frey and Smith (2007) mentioned insufficient accuracy of WS wetland maps with the best agreement of only 56 % for the high-resolution WS Peatland Database (WSLPD) (Sheng et al., 2004). Coarse-resolution products tend to underestimate the wetland area when the water table is a few centimetres below the moss cover, resulting in the conclusion that surface is not saturated with water (Saarnio et al., 1997; Friborg et al., 2003; Krankina et al., 2008).

Modellers should be able to draw upon a global version of the high-resolution map that not only delineates wetlands but also identifies the major sub-types to which different environmental parameters could potentially be applied (Bohn et al., 2015). Various wetland maps have been used to define the wetland extent in WS, however simplistic classification schemes in aggregate to limited or no ground truth data and strong generalization of classes diminish their applicability. The only peatland typology map that distinguishes several vegetation and microtopography classes and their mixtures was developed at the State Hydrological Institute (SHI) by Romanova et al. (1977). Peregon et al. (2005) digitized and complemented this map by estimating the fractional coverage of wetland structural components or wetland ecosystems using Landsat and high-resolution images for five test sites. However, the limited amount of fractional coverage data and coarse resolution introduce large uncertainties in scaled-up estimations (Kleptsova et al., 2012).





BGD
12, 20149–20178, 2015

Our long-term goal is to develop a multi-scale approach for mapping Russian wetlands using Landsat imagery with a resolution of 30 m so that the results can better meet the needs of land process modelling and other applications concerning methane emissions from peatlands. In this study, the WS taiga zone was chosen as the primary target for the land cover classification due to the abundance of wetlands. The objectives were threefold: first, develop a consistent land cover of peatland classes and its structural components; second, understand the spatial distribution of different wetlands and their linkage with other land units; and third, provide the foundation for environmental parameter upscaling and the model assessment.

## 2 Materials and methods

### 2.1 Study region

The West Siberian Lowland is a geographical region of Russia bordered by the Urals in the west and the Yenisey River in the east; the region covers 275 Mha stretching from 62–89° E to 53–73° N. Because of its great expanse and flat topography, the vegetation cover of the Lowland has clear latitudinal zonation. According to Gvozdetsky (1968), the taiga zone is divided into three geobotanical subzones: northern taiga, middle taiga and southern taiga. It corresponds to the raised string bog province and covers about 160 Mha in the central part of the WS. It is characterized by flat topography with elevations of 80 to 100 m a.s.l. rising to about 190 m in the "Siberian Uvaly" area. Average annual precipitation is about 450–500 mm and evaporation is 200–400 mm (Rihter, 1963). The excess water supply and flat topography with impeded drainage provides favourable conditions for wetland formation. Large fraction of the area, including watersheds and floodplains, is waterlogged. The hydrographic structure of this zone differs from the northern and southern parts of the WS. The largest peatlands are most typical of the central flat parts of the watersheds where, together with forests, they comprise the zonal vegetation and cover vast territories (Solomeshch, 2005). Com-





BGD
12, 20149–20178, 2015

prehensive synthesis of Russian literature regarding the current state of the WS peatlands, their development and sensitivity to climatic changes was made by Kremenetski et al. (2003). The study summarizes information about WS geology, hydrology, climate, vegetation, and peatland zonation. Basing on existing Russian data, authors found that the mean depth of peat accumulation in the WSL is 256 cm and the total amount of carbon stored there may exceed $54 \times 10^9$ metric tons.

## 2.2 Classification methodology

No single classification algorithm can be considered as optimal methodology for improving vegetation discrimination and mapping; hence, the use of advanced classifier algorithms must be based on their suitability to achieve certain objectives in specific areas (Adam et al., 2009). Because mapping over large landscapes typically involves many satellite scenes, multi-scene mosaicking is often used to group scenes into a single file for further classification. This approach optimizes both the classification process and edge matching. However, large multi-scene mosaicking has essential drawback when applying to highly heterogeneous WS wetlands. It creates a variety of spectral gradients within the file (Homer and Gallant, 2001), especially when the number of the appropriate scenes with similar vegetation and hydrological conditions is limited. As a result, spectral discrepancy that is difficult to overcome emerges even within wetland types. In this study, it was considered that the advantages of consistency in class definition within scene-by-scene classification greatly exceed the disadvantages of edge matching and processing slowness. Thus, our entire analysis was performed on a scene-by-scene basis, as conducted by Giri et al. (2011) and Gong et al. (2013).

The scene selection procedure was facilitated because the possibility to adequately smooth the slight inconsistencies between images by specifying training sites in overlapped areas. Ideally, it is better to use data acquired in the same year or season, especially in the peak of the growing season (July), for wetland identification. However, the main complication was the low accessibility of good quality cloudless images of WS from those periods. Scenes collected earlier than the 2000s were considered outdated due to land cover changes, so they were used as substitutes for places where no suitable imagery could be found. Landsat-7 images received after 2003 were not used due to data gaps, and Landsat-8 was launched after the beginning mapping procedure. Finally, we collected 70 compatible vegetation scenes during the peak of the growing seasons in different years. Majority of the images were from 2007.

The overall work flow involves data pre-processing, training and test sample collection, image classification on a scene-by-scene basis, the regrouping of the derived classes into 9 wetland complexes, the estimation of wetland ecosystem fractional coverage and accuracy assessment. Atmospheric correction was not applied because this process is unnecessary as long as the training data are derived from the image being classified (Song et al., 2001). All of the images were re-projected onto the Albers projection. Because the vegetation of the West Siberian plane includes various types of forests, meadows, burned areas, agricultural fields, etc., wetland environments were distinguished from other landscapes using a thresholding method to avoid misclassification. We used the Green-Red Vegetation Indices (Motohka et al., 2010) to separate majority of wetlands and forests; the 5th Landsat channel was used to mask the most inundated areas including water bodies. These thresholds were empirically determined for each scene by testing various candidate values in Quantum GIS. Masked Landsat images were filtered in MATLAB v.7.13 (MathWorks) to remove random noise and then classified in Multispec v.3.3 (Purdue Research Foundation) using a supervised classification method. The maximum likelihood algorithm was used because of its robustness and availability in almost any image-processing software (Lu and Weng, 2007). All bands except the thermal infrared band were used.

Training data plays a critical role in the supervised classification technique. Representative data collection is the most time-consuming and labour-intensive process in regional scale mapping efforts (Gong et al., 2013). Due to the remoteness of WS, we have a lack of ground truth information, which hampers training dataset construction. As a result, we were constrained to base training sample selections mostly on high-resolution imagery available in Google Earth. Our field knowledge comprising 8 years of fieldwork in West Siberia, which resulted in an extensive dataset of botanical descriptions, field photos, and pH and electrical conductivity data from 28 test sites (Glagolev et al., 2011). They were used as an additional source of information. The processing started with mapping scenes where ground truth data and high-resolution images are extensively available, so the classification results could be checked for quality assurance, continued through contiguous images and ended at the less explored scenes with poor ground truth and auxiliary data coverage. To collect training data most efficiently, we used criteria similar to those in (Gong et al., 2013) for training sample selection: (i) the training samples must be homogeneous; land-cover mixtures and heterogeneous areas are avoided, and (ii) all of the samples must be at least 10 pixels in size with an average sample area of approximately 100–200 pixels.

The spectral classes that were discriminated during the supervised classification were generalized into 9 wetland complexes. Classification mismatch in overlapping areas was minimized by collecting training samples from overlapping areas until satisfactory results were achieved. Because temporal differences exist among the scenes, patch effects can be slightly observed. Classified images and area calculations were combined using the GRASS module in Quantum GIS. Wetlands and water bodies that are only one or a few Landsat pixels in size exist, and some of these sites may be random image noises. Therefore, a simple low pass filter was applied to eliminate such objects.

### 2.3 Wetland typology development

As a starting point for the mapping procedure, a proper classification scheme is required. Congalton et al. (2014) showed that the classification scheme has the highest error contribution and implementation priority. Its development relies on the study purposes and the class separability of the input variables. In our case, wetland mapping was initially conceived as an advanced technique to improve the estimation of the regional $CH_4$ flux and, secondarily, as a base to upscale other ecological functions. WS wetlands are heterogeneous with highly variable water table levels (WTL), geochemical conditions, vegetation covers, etc. However, these wetlands are composed of relatively homogeneous structural elements or "wetland ecosystems" with similar environmental features and, thus, rates of $CH_4$ emissions (Sabrekov et al., 2013). To yield reliable upscaling, we assigned 7 wetland ecosystems in our classification scheme (Fig. 1):

1. "Water": all water bodies greater than 2 × 2 Landsat pixels;
2. "waterlogged hollows": water bodies fewer than 2 × 2 Landsat pixels or depressed parts of wetland complexes with WTLs above the average moss/vegetation surface;
3. "oligotrophic hollows": depressed parts of bogs with WTLs beneath the average moss/vegetation cover;
4. "ridges": long and narrow elevated parts of wetland complexes with dwarf shrubs-sphagnum vegetation cover;
5. "ryams": extensive pine-dwarf shrubs-sphagnum peatland areas;
6. "fens": integrated class for various types of rich fens, poor fens and wooded swamps;
7. "palsa hillocks": elevated parts of palsa complexes with permafrost below the surface.

However, wetland ecosystems generally have sizes of approximately 1–10 m and cannot be directly distinguished using Landsat imagery with 30 m resolutions, with a few exceptions. When the objects in the scene become increasingly smaller relative to the resolution cell size, they may no longer be regarded as individual objects. The reflectance measured by the sensor can be treated as a sum of the interactions among various classes of scene elements as weighted by their relative proportions (Lu and Weng, 2007; Strahler et al., 1986). Therefore, we developed a second wetland typology that involves 9 mixed "wetland complexes" and then estimated the fractional area coverage of the wetland ecosystems within each of them (Fig. 1; Table 1). The assigned wetland complexes should meet the following criteria: (i) distinguishability by Landsat images, and (ii) abundance in the WS taiga zone. All these complexes were described in detail in a number of Russian studies (Katz and Neishtadt, 1963; Walter, 1977; Romanova, 1985; Liss et al., 2001; Lapshina, 2004; Solomeshch, 2005; Usova, 2009; Masing et al., 2010) and encompass wooded, patterned, open wetlands and water bodies.

To estimate the fractional area coverage of the wetland ecosystems, we selected 8–27 test sites of 0.1–1 $km^2$ size for each wetland complex depending on its heterogeneity. High-resolution images corresponding to these areas were classified in Multispec v.3.3 by an unsupervised classification method. Finally, the obtained wetland ecosystem ratios were averaged among the test sites. This approach is similar to the method described by Peregon et al. (2005), where the evaluation of the area fraction occupied by "micro-landscape" elements within patterned wetlands was based on aerial photography.

During wetland typology development, we were forced to make several assumptions. First, the wetland complexes were considered individual objects, while they actually lie along a continuum, have vague borders (Fig. 1) and floating ratios of wetland ecosystems. Second, the classification schemes include all water bodies, although many (rivers, creeks, and large lakes) are not structural components of wetlands. Based on field knowledge, we assumed that all of the water bodies that arose from peatland development have sizes less than 2 × 2 Landsat pixels. These water bodies are represented by wetland pools, waterlogged hollows and watercourses, which are structural components of RHLC. The rest of the water bodies were placed into the "Lakes and rivers" class. Third, in this study, we only consider peatlands and water bodies; floodplain areas were not taken into account aside from misclassification cases.





BGD
12, 20149–20178, 2015

## 3 Results and discussion

### 3.1 Wetland map

Using Landsat imagery, we developed a high-resolution wetland inventory of the WS taiga zone (Fig. 2). The total area of wetlands and water bodies was estimated to be 52.4 Mha. West Siberian taiga wetlands proved to be noticeable even at the global scale. Based on observational datasets, the global average of inundated areas and peatlands was assumed to cover from 430 (Cogley, 1994) to 1170 Mha (Lehner and Döll, 2004) as summarized by Melton et al. (2013); therefore, taiga wetlands in WS account for approximately 4–12 % of the total wetland area. Their coverage is larger than the total wetland areas of 32.4, 32, and 41 Mha in China (Niu et al., 2012), Hudson Bay Lowland (Cowell, 1982) and Alaska (Whitcomb et al., 2009), respectively. The extent of West Siberia's wetlands exceeds the tropical wetland area of 43.9 Mha (Page et al., 2011), emphasizing the considerable ecological role of the studied region.

As summarized by Sheng et al. (2004), the majority of previous local Russian studies estimated the extent of the entire WS's mires to be much lower. These studies probably inherited the drawbacks of the original Russian Federation Geological Survey database, which was used as the basis for the existing WS peatland inventories (Ivanova and Novikova, 1976). This database was characterized by a lack of field data in remote regions and a high generalization level and only considers economically valuable wetlands with peat layers deeper than 50 cm.

Our peatland coverage is most similar to the estimate of 51.5 Mha (Peregon et al., 2009) by SHI map (Romanova et al., 1977). However, a direct comparison between the peatland structures shows that the SHI map is too generalized without sufficient detail on the wetland distribution (Fig. 3). SHI map was based on aerial photography, which is not feasible for mapping and monitoring wetland vegetation on a regional scale because it is too costly and time-consuming to process (Adam et al., 2009). The satellite-based classifications tend to identify many small peatlands and their subgroups, which are ignored in the more generalized SHI map. However, the satellite classifications also





BGD
12, 20149–20178, 2015

delineate small gaps within contiguous peatlands. The net result of both effects is a fortuitous cancellation of their differences (Sheng et al., 2004), leaving the discrepancy in the spatial distributions. The latter is essential for environmental parameter upscaling purposes. In the case study of WS's middle taiga, we found that applying the new wetland map led to a 130 % increase in the $CH_4$ flux estimation from the domain (Kleptsova et al., 2012) comparing with estimation based on SHI map. Thus, a considerable revaluation of the total $CH_4$ emissions from the whole region is expected.

### 3.2 Regularities of zonal distribution

WS has a large variety of wetlands that developed under different climatic and geomorphologic conditions. Concerning the wetland complex typology (excluding the "Lakes and rivers" class), RHCs prevail in WS's taiga, occupying 32.2 % of the domain, followed by ryams (23 %), RHLCs (16.4 %), open fens (8.4 %), palsa complexes (7.6 %), open bogs (4.8 %), patterned fens (3.9 %) and swamps (3.7 %). Various oligotrophic environments are dominant among the wetland ecosystems (Table 2), while fens cover only 14.3 % of the wetlands. Waterlogged hollows and open water occupy 7 % of the region, which is similar to the average estimation by Watts et al. (2014), who found that 5 % of the boreal-Arctic domain was inundated with surface water during the non-frozen summer season.

The individual wetland environments have a strongly pronounced latitudinal zonality within the studied region. Zonal borders stretch closely along latitude lines, subdividing the taiga domain into the southern, middle, and northern taiga subzones (Fig. 2, black lines). The knowledge regarding the spatial distribution of different wetlands facilitates mapping and further understanding of their linkage with each other and other land units. To visualize the regularities of the wetland distribution, we divided the entire area into $0.1^{\circ} \times 0.1^{\circ}$ grids and calculated the wetland ecosystem to the total cell area ratios for each grid (Fig. 4) using fractional coverage data from Table 1. A slight patch effect that ensues from the scene-by-scene classification technique is observed. Abrupt leaps





BGD
12, 20149–20178, 2015

correspond to classification errors and indicate less accurate map patches, which can be improved by more careful image acquisition.

WS's northern taiga (approximately 62–65° N) has approximately 36 % mire coverage. Because of the abundance of precipitation, minimal evaporation, and scanty runoff, the northern taiga corresponds to the maximal distribution of lakes and waterlogged hollows, covering a third of the domain (Fig. 4a and b). Vast parts of the zone are occupied by the peatland system "Surgutskoe Polesye," which stretches for a hundred kilometres from east to west and is located between 61.5 and 63° N. Peatland and water bodies cover up to 70 % of the territory, forming several huge peatland-lake complexes that are divided by river valleys. Northward, the slightly paludified "Siberian Elevation" (63.5° N) divides the northern taiga into two lowland parts. Palsa hillocks appear in the "Surgutskoe Polesye" region and replace the ridges and ryams to the north of the "Siberian Elevation" region (Fig. 4f).

RHCs are the most abundant in the middle taiga (approximately 59–62° N), where mires occupy 34 % of the area. Large wetland systems commonly cover watersheds and have a convex cupola with centres that are 3 to 6 m higher than the periphery. These environments have peat layers that are several meters deep and are composed of sphagnum peat with the small addition of other plants. The wetland ecosystems here have strict spatial regularities. Central plateau depressions with stagnant water are represented by RHLCs. Different types of RHCs cover better-drained gentle slopes. The most drained areas are dominated by ryams. Poor and rich fens develop along the wetland's edges, with low lateral water flow and relatively high nutrient availability. Wooded swamps usually surround peatland systems.

The wetland extent reaches 28 % in WS's southern taiga area (approximately 56–59° N). Vast peatland systems are composed of raised bogs represented by ryams and RHCs with huge open and patterned fens between them. The eastern part of the subzone is dominated by small and medium-sized wetland complexes. The southern taiga wetlands have similar spatial regularities as the middle taiga; however, the area of the fens increases stepwise here due to the abundance of carbonate soils and the





BGD
12, 20149–20178, 2015

higher nutrient availability. Velichko et al. (2011) provided evidence of a vast cold desert in the northern half of WS during the last glacial period, while the southernmost part of the plain was an area of loess accumulation. Now, the border between fen and bog dominated areas extends near 59° N and corresponds to the border between the southern and middle taiga zones (Fig. 4c and e).

### 3.3 Accuracy assessment

The accuracy assessment was based on 1082 validation polygons of 10 × 10 pixels that were randomly spread over the WS taiga zone. We used high-resolution images available in Google Earth as ground truth information. The confusion matrix (Table 3) was used as an effective way to represent map accuracy as the individual accuracies of each category are plainly described along with both the errors of inclusion and errors of exclusion (Congalton and Green, 2008). We found that the accuracies for different land-cover categories varied from 62 to 99 %, with the lake and river, ryam, and RHC areas classified the best and open bogs and patterned fens the most confused. Misclassifications usually occurred between neighbouring classes with greater similarities in their environmental parameters, which exhibit only minor distortions in map applications. Some errors occurred along boundaries and were associated with mixed pixels (33 polygons), whose presence had been recognized by Foody (2002) as a major problem, affecting the effective use of remotely sensed data in per-pixel classification.

Wetland complexes within large wetland systems have high classification accuracies. In contrast, our approach omits wetlands below a certain size, and the uncertainties are particularly high for the smallest objects. Great effort was exerted to map the individual wetlands that are abundant in the southern part of the domain due to the prevalence of agricultural fields. We tested several vegetation indices until the Landsat thermal band was revealed to produce the optimal thresholding results due to its ability to estimate the soil moisture. Many of the errors were also disposed along the tundra boundary, related to the lack of ground truth data and worsened by the high landscape heterogeneity. However, those small areas do not make a substantial difference in the global total.

Among the classes, patterned fens and open bogs were classified with the lowest producer's accuracy (PA), which was 62 %. Patterned fens include substantial treeless areas, so they were often misclassified as open fens. They were also confused with RHCs due to the similar "ridge-hollow" structure. Open bogs often have tussock shrub cover with sparse pines, increasing the frequency of misclassification as RHCs and ryams. Open fens have higher user's accuracy (UA) and PA; however, these values were probably overestimated. High-resolution images poorly reflect nutrient supply levels, which underrates the classification errors between open bogs and open fens. Swamps and palsa complexes have very high PA and low UA, which is related to their incorrect identification in non-wetland areas. Palsa complexes were spectrally close to open woodlands, with pine and lichen vegetation covering wide portions of northern WS. Swamps were commonly confused with forests; in dry periods, they can be recognized mainly by the field investigations based on the typical microrelief and presence of peat layers. In both cases, more accurate wetland masks would lead to substantially higher accuracy levels. Lakes and rivers were classified the best due to the high spectral separability of the class. They can be seldom confused with RHLCs, especially when represented by a series of small lakes or waterlogged hollows that are divided by narrow necks on the land. Floodplains can also be classified as lakes and rivers when the image corresponds to the most inundated period after snow melting (11 polygons). RHCs and ryams were accurately identified due to the abundance of these categories in the study region and their high spectral separability.

Generally, we indicate a reasonable accuracy of 79 % for such a large and remote area. However, this value seems to be slightly overestimated, because high-resolution images are not always effective in distinguishing similar environments that differ in their nutrient supply level.





BGD
12, 20149–20178, 2015

### 3.4 Challenges and future prospects

The spectral discrimination of wetland types in complex environments is a challenging task because different vegetation types commonly possess the same spectral signature in remotely sensed images (Ozesmi and Bauer, 2002; Xie et al.). However, the contrast between vast wetland systems and the surrounding forest areas is usually so distinct that wetlands can be adequately identified by the summer season images, in which the discrimination between wetlands and forests does not impose a serious problem (Sheng et al., 2004). On the contrary, correctly distinguishing continuous series of wetland complexes complicated by seasonal variations remain one of the largest challenges. Wetlands become the most inundated after snow melting or long rainy periods, resulting in the transformation of oligotrophic hollows and fens into waterlogged hollows. Thus, RHCs or patterned fens can turn into RHLC because of flooding (Fig. 1: areas in RHCs with brown Sphagnum cover usually turn into waterlogged hollows after flooding). Swamps commonly dry up after drought periods, and their environmental features become similar to those of non-wetland areas. Oppositely, the huge floodplains of the Ob' and Irtysh Rivers become inundated during prolonged snowmelt floods. Interannual variability also occurs in WS (Schroeder et al., 2010; Watts et al., 2014). The changes in water level are especially reasonable for $CH_4$ flux upscaling purposes because the areal extent of methane-emitting regions across the landscape, and therefore, the total methane emissions, is a function of the spatial distribution of water table depths (Bohn et al., 2007). Watts et al. (2014) underscored the importance of monitoring changes in surface moisture and temperature when assessing the vulnerability of boreal-Arctic wetlands to enhanced greenhouse gas emissions under a shifting climate.

New methodologies and protocols are needed to combine remotely sensed observations to improve our ability to monitor continuous water levels or distinguish habitat types or other characteristics of wetland environments (Kim et al., 2009). Perhaps the best opportunity in the next few years for routine measurements of inundated areas will





BGD
12, 20149–20178, 2015

result from PALSAR. The use of additional radar data to map the most inundated areas will be especially useful for $CH_4$ flux upscaling because only wetland ecosystems with high water levels contribute to the regional flux, while the effects of dryer ecosystems (ryams, ridges and palsa hillocks) can be neglected (Glagolev et al., 2011; Sabrekov et al., 2014).

Although the synergistic combination of optical and radar data is advantageous for accurately characterizing open water (Schroeder et al., 2010) and wetlands, the remote sensing of water regimes is successful only when in situ data are available for calibration. We still lack in situ measurements of the water table dynamics and extent in WS's wetlands. Simplistic monitoring measurements have been made at the Bakchar field station (Krasnov et al., 2013) and Mukhrino field station (Bleuten and Filippov, 2008); however, the vast majority of obtained data were not published. These measurements are of special importance for the northern taiga zone, where small shallow lakes and waterlogged hollows with fluctuating water regimes cover huge areas.

The scarcity of reliable reference data and subsequent lack of consistency limit the accuracy of land cover information that are derived from satellite imagery (Homer and Gallant, 2001). The use of ancillary data can largely improve the accuracy of maps (Congalton et al., 2014); however, more reliable classification accuracy comes with significant costs regarding data, local knowledge, and detailed field data. The next step in improving mapping should rely on the acquisition of ground truth data from the most ambiguous wetland landscapes and remote regions.

## 4 Conclusions

Boreal peatlands play a major role in carbon storage, methane emissions, water cycling and other global environmental processes, but better understanding of this role is constrained by the inconsistent representation of peatlands on (or even complete omission from) many global land cover maps (Krankina et al., 2008). In this study, we describe a map representing the state of the taiga wetlands in WS during the peak of





BGD
12, 20149–20178, 2015

the growing season. Although Hansen and Loveland (2012) highlighted that “per scene, interactive analyses will no longer be viable” for global land cover studies; however, we still find that the procedure is quite suitable for regional mapping with highly heterogeneous landscapes and low accessibility of good quality cloudless images. The efforts reported here can be considered as an initial attempt at mapping Russian wetlands using Landsat imagery, with the general goal of supporting the monitoring of wetland resources and upscaling the methane emissions from wetlands and inland waters. The resulting quantitative definitions of wetland complexes combined with a new wetland map can be used for the estimation and spatial extrapolation of many ecosystem features to the regional scale. In the case study of WS's taiga, applying a new wetland map led to a significant change in the wetland ecosystem areas comparing to the estimate by Peregon et al. (2009), previously used in our methane inventory (Glagolev et al., 2011). Thus, a considerable revaluation of the total $CH_4$ emissions from the entire region is expected.

We estimate a map accuracy of 79 %, which is reasonably good for this large and remote area. The next step in improving mapping quality will depend on the acquisition of ground truth data from the most ambiguous wetland landscapes and remote regions. Correctly distinguishing wetland complexes with strongly pronounced seasonal variability in their water regimes, remains one of the largest challenges. There is a need for installing water level gauge network embracing at least most abundant wetland types.

Our new Landsat-based map of WS's taiga wetlands provides a benchmark for validation of coarse-resolution global land cover products and for assessment of global model performance in high latitudes. Classification scheme was oriented on methane inventory but is applicable for the upscaling of other environmental parameters.

*Acknowledgements.* We thank Amber Soja for assisting in evaluating the initial version of the manuscript. This study (research grant No 8.1.94.2015) was supported by The Tomsk State University Academic D.I. Mendeleev Fund Program in 2014–2015. The study was also supported by the GRENE-Arctic project by MEXT Japan and by RFBR, research projects No. 15-05-07622 and 15-44-00091.

## References

Adam, E., Mutanga, O., and Rugege, D.: Multispectral and hyperspectral remote sensing for identification and mapping of wetland vegetation: a review, Wetl. Ecol. Manag., 18, 281–296, doi:10.1007/s11273-009-9169-z, 2009.

Bleuten, W. and Filippov, I.: Hydrology of mire ecosystems in central West Siberia: the Mukhrino Field Station, in: Transactions of UNESCO department of Yugorsky State University "Dynamics of environment and global climate change", edited by: Glagolev, M. V. and Lapshina, E. D., NSU, Novosibirsk, Russia, 208–224, 2008.

Bohn, T. J., Lettenmaier, D. P., Sathulur, K., Bowling, L. C., Podest, E., McDonald, K. C., and Friborg, T.: Methane emissions from western Siberian wetlands: heterogeneity and sensitivity to climate change, Environ. Res. Lett., 2, 045015, doi:10.1088/1748-9326/2/4/045015, 2007.

Bohn, T. J., Melton, J. R., Ito, A., Kleinen, T., Spahni, R., Stocker, B. D., Zhang, B., Zhu, X., Schroeder, R., Glagolev, M. V., Maksyutov, S., Brovkin, V., Chen, G., Denisov, S. N., Eliseev, A. V., Gallego-Sala, A., McDonald, K. C., Rawlins, M. A., Riley, W. J., Subin, Z. M., Tian, H., Zhuang, Q., and Kaplan, J. O.: WETCHIMP-WSL: intercomparison of wetland methane emissions models over West Siberia, Biogeosciences Discuss., 12, 1907–1973, doi:10.5194/bgd-12-1907-2015, 2015.

Bridgham, S. D., Cadillo-Quiroz, H., Keller, J. K., and Zhuang, Q.: Methane emissions from wetlands: biogeochemical, microbial, and modeling perspectives from local to global scales, Glob. Change Biol., 19, 1325–1346, doi:10.1111/gcb.12131, 2013.

Cogley, J.: GGHYDRO: global hydrographic data, Peterborough, Ontario, Canada, 1994.

Congalton, R., Gu, J., Yadav, K., Thenkabail, P., and Ozdogan, M.: Global land cover mapping: a review and uncertainty analysis, Remote Sensing, 6, 12070–12093, doi:10.3390/rs61212070, 2014.

Congalton, R. G. and Green, K.: Assessing the Accuracy of Remotely Sensed Data: Principles and Practices, CRC Press, Boca Raton, Florida, USA, 2008.

Cowell, D. W.: Earth Sciences of the Hudson Bay Lowland: Literature Review and Annotated Bibliography, Lands Directorate, Environment Canada, Burlington, Ontario, Canada, 1982.

Eppinga, M. B., Rietkerk, M., Belyea, L. R., Nilsson, M. B., Ruiter, P. C. D., and Wassen, M. J.: Resource contrast in patterned peatlands increases along a climatic gradient, Ecology, 91, 2344–2355, 2010.

Foody, G. M.: Status of land cover classification accuracy assessment, Remote Sens. Environ., 80, 185–201, 2002.
Frey, K. E. and Smith, L. C.: How well do we know northern land cover?, Comparison of four global vegetation and wetland products with a new ground-truth database for West Siberia, Global Biogeochem. Cy., 21, GB1016, doi:10.1029/2006gb002706, 2007.
Friborg, T., Soegaard, H., Christensen, T. R., Lloyd, C. R., and Panikov, N. S.: Siberian wetlands: where a sink is a source, Geophys. Res. Lett., 30, 2129, doi:10.1029/2003GL017797, 2003.
Giri, C., Ochieng, E., Tieszen, L. L., Zhu, Z., Singh, A., Loveland, T., Masek, J., and Duke, N.: Status and distribution of mangrove forests of the world using earth observation satellite data, Global Ecol. Biogeogr., 20, 154–159, doi:10.1111/j.1466-8238.2010.00584.x, 2011.
Glagolev, M., Kleptsova, I., Filippov, I., Maksyutov, S., and Machida, T.: Regional methane emission from West Siberia mire landscapes, Environ. Res. Lett., 6, 045214, doi:10.1088/1748-9326/6/4/045214, 2011.
Gong, P., Wang, J., Yu, L., Zhao, Y., Zhao, Y., Liang, L., Niu, Z., Huang, X., Fu, H., Liu, S., Li, C., Li, X., Fu, W., Liu, C., Xu, Y., Wang, X., Cheng, Q., Hu, L., Yao, W., Zhang, H., Zhu, P., Zhao, Z., Zhang, H., Zheng, Y., Ji, L., Zhang, Y., Chen, H., Yan, A., Guo, J., Yu, L., Wang, L., Liu, X., Shi, T., Zhu, M., Chen, Y., Yang, G., Tang, P., Xu, B., Giri, C., Clinton, N., Zhu, Z., Chen, J., and Chen, J.: Finer resolution observation and monitoring of global land cover: first mapping results with Landsat TM and ETM+ data, Int. J. Remote Sens., 34, 2607–2654, doi:10.1080/01431161.2012.748992, 2013.
Gvozdetsky, N.: Physiographic zoning of USSR, MSU, Moscow, Russia, 576 pp., 1968.
Hansen, M. C. and Loveland, T. R.: A review of large area monitoring of land cover change using Landsat data, Remote Sens. Environ., 122, 66–74, doi:10.1016/j.rse.2011.08.024, 2012.
Homer, C. and Gallant, A.: Partitioning the Conterminous United States into Mapping Zones for Landsat TM Land Cover Mapping, unpublished US Geologic Survey report, 2001.
Ivanova, K. and Novikova, S.: West Siberian Peatlands, Their Structure and Hydrological Regime, Gidrometeoizdat, Leningrad, USSR, 448 pp., 1976.
Katz, N. and Neishtadt, M.: Peatlands, in: West Siberia, edited by: Rihter, G. D., AS USSR, Moscow, Russia, 230–248, 1963.
Kim, J.-W., Lu, Z., Lee, H., Shum, C. K., Swarzenski, C. M., Doyle, T. W., and Baek, S.-H.: Integrated analysis of PALSAR/Radarsat-1 InSAR and ENVISAT altimeter data for mapping of absolute water level changes in Louisiana wetlands, Remote Sens. Environ., 113, 2356–2365, doi:10.1016/j.rse.2009.06.014, 2009.

Kleptsova, I., Glagolev, M., Lapshina, E., and Maksyutov, S.: Landcover classification of the Great Vasyugan mire for estimation of methane emission, in: 1st International Conference on "Global Warming and the Human-Nature Dimension in Siberia: Social Adaptation to the Changes of the Terrestrial Ecosystem, with an Emphasis on Water Environments", 7–9 March 2012, Kyoto, Japan, 38–41, 2012.

Krankina, O. N., Pflugmacher, D., Friedl, M., Cohen, W. B., Nelson, P., and Baccini, A.: Meeting the challenge of mapping peatlands with remotely sensed data, Biogeosciences, 5, 1809–1820, doi:10.5194/bg-5-1809-2008, 2008.

Krasnov, O. A., Maksutov, S. S., Glagolev, M. V., Kataev, M. Y., Inoue, G., Nadeev, A. I., and Schelevoi, V. D.: Automated complex "Flux-NIES" for measurement of methane and carbon dioxide fluxes, Atmospheric and Oceanic Optics, 26, 1090–1097, 2013.

Kremenetski, K. V., Velichko, A. A., Borisova, O. K., MacDonald, G. M., Smith, L. C., Frey, K. E., and Orlova, L. A.: Peatlands of the Western Siberian lowlands: current knowledge on zonation, carbon content and Late Quaternary history, Quaternary Sci. Rev., 22, 703–723, doi:10.1016/s0277-3791(02)00196-8, 2003.

Lapshina, E.: Peatland Vegetation of South-East West Siberia, TSU, Tomsk, Russia, 296 pp., 2004.

Lehner, B. and Döll, P.: Development and validation of a global database of lakes, reservoirs and wetlands, J. Hydrol., 296, 1–22, doi:10.1016/j.jhydrol.2004.03.028, 2004.

Liss, O., Abramova, L., Avetov, N., Berezina, N., Inisheva, L., Kurnishkova, T., Sluka, Z., Tolpysheva, T., and Shvedchikova, N.: Mire Systems of West Siberia and Its Nature Conservation Importance, Grif and Co, Tula, Russia, 584 pp., 2001.

Lu, D. and Weng, Q.: A survey of image classification methods and techniques for improving classification performance, Int. J. Remote Sens., 28, 823–870, doi:10.1080/01431160600746456, 2007.

Masing, V., Botch, M., and Läänelaid, A.: Mires of the former Soviet Union, Wetl. Ecol. Manag., 18, 397–433, 2010.

Melton, J. R., Wania, R., Hodson, E. L., Poulter, B., Ringeval, B., Spahni, R., Bohn, T., Avis, C. A., Beerling, D. J., Chen, G., Eliseev, A. V., Denisov, S. N., Hopcroft, P. O., Lettenmaier, D. P., Riley, W. J., Singarayer, J. S., Subin, Z. M., Tian, H., Zürcher, S., Brovkin, V., van Bodegom, P. M., Kleinen, T., Yu, Z. C., and Kaplan, J. O.: Present state of global wetland extent and wetland methane modelling: conclusions from a model inter-comparison project (WETCHIMP), Biogeosciences, 10, 753–788, doi:10.5194/bg-10-753-2013, 2013.

Motohka, T., Nasahara, K. N., Oguma, H., and Tsuchida, S.: Applicability of green-red vegetation index for remote sensing of vegetation phenology, Remote Sensing, 2, 2369–2387, 2010.

Niu, Z., Zhang, H., Wang, X., Yao, W., Zhou, D., Zhao, K., Zhao, H., Li, N., Huang, H., Li, C., Yang, J., Liu, C., Liu, S., Wang, L., Li, Z., Yang, Z., Qiao, F., Zheng, Y., Chen, Y., Sheng, Y., Gao, X., Zhu, W., Wang, W., Wang, H., Weng, Y., Zhuang, D., Liu, J., Luo, Z., Cheng, X., Guo, Z., and Gong, P.: Mapping wetland changes in China between 1978 and 2008, Chinese Sci. Bull., 57, 2813–2823, doi:10.1007/s11434-012-5093-3, 2012.

Ozesmi, S. L. and Bauer, M. E.: Satellite remote sensing of wetlands, Wetl. Ecol. Manag., 10, 381–402, 2002.

Page, S. E., Rieley, J. O., and Banks, C. J.: Global and regional importance of the tropical peatland carbon pool, Glob. Change Biol., 17, 798–818, 2011.

Peregon, A., Maksyutov, S., Kosykh, N., Mironycheva-Tokareva, N., Tamura, M., and Inoue, G.: Application of the multi-scale remote sensing and GIS to mapping net primary production in west Siberian wetlands, Phyton, 45, 543–550, 2005.

Peregon, A., Maksyutov, S., Kosykh, N. P., and Mironycheva-Tokareva, N. P.: Map-based inventory of wetland biomass and net primary production in western Siberia, J. Geophys. Res.-Biogeo., 113, G01007, doi:10.1029/2007JG000441, 2008.

Peregon, A., Maksyutov, S., and Yamagata, Y.: An image-based inventory of the spatial structure of West Siberian wetlands, Environ. Res. Lett., 4, 045014, doi:10.1088/1748-9326/4/4/045014, 2009.

Petrescu, A. M. R., van Beek, L. P. H., van Huissteden, J., Prigent, C., Sachs, T., Corradi, C. A. R., Parmentier, F. J. W., and Dolman, A. J.: Modeling regional to global $CH_4$ emissions of boreal and arctic wetlands, Global Biogeochem. Cy., 24, doi:10.1029/2009gb003610, 2010.

Rihter, G. D.: West Siberia, AS USSR, Russia, Moscow, 1963.

Romanova, E., Bybina, R., Golitsyna, E., Ivanova, G., Usova, L., and Trushnikova, L.: Wetland typology map of West Siberian lowland scale 1 : 2500000 GUGK, Leningrad, Russia, 1977.

Romanova, E.: Vegetation cover of West Siberian Lowland, in: Peatland Vegetation, edited by: Il'ina, I., Lapshina, E., Lavrenko, N., Meltser, L., Romanove, E., Bogoyavlenskiy, M., and Mahno, V., Science, Novosibirsk, Russia, 138–160, 1985.





BGD
12, 20149–20178, 2015

Saarnio, S., Alm, J., Silvola, J., Lohila, A., Nykänen, H., and Martikainen, P. J.: Seasonal variation in $CH_4$ emissions and production and oxidation potentials at microsites on an oligotrophic pine fen, Oecologia, 110, 414–422, 1997.

Sabrekov, A., Glagolev, M., Kleptsova, I., Machida, T., and Maksyutov, S.: Methane emission from mires of the West Siberian taiga, Eurasian Soil Sci., 46, 1182–1193, 2013.

Sabrekov, A. F., Runkle, B. R. K., Glagolev, M. V., Kleptsova, I. E., and Maksyutov, S. S.: Seasonal variability as a source of uncertainty in the West Siberian regional $CH_4$ flux upscaling, Environ. Res. Lett., 9, 045008, doi:10.1088/1748-9326/9/4/045008, 2014.

Schroeder, R., Rawlins, M. A., McDonald, K. C., Podest, E., Zimmermann, R., and Kueppers, M.: Satellite microwave remote sensing of North Eurasian inundation dynamics: development of coarse-resolution products and comparison with high-resolution synthetic aperture radar data, Environ. Res. Lett., 5, 015003, doi:10.1088/1748-9326/5/1/015003, 2010.

Sheng, Y., Smith, L. C., MacDonald, G. M., Kremenetski, K. V., Frey, K. E., Velichko, A. A., Lee, M., Beilman, D. W., and Dubinin, P.: A high-resolution GIS-based inventory of the west Siberian peat carbon pool, Global Biogeochem. Cy., 18, GB3004, doi:10.1029/2003gb002190, 2004.

Solomeshch, A.: The West Siberian Lowland, The World's Largest Wetlands: Ecology and Conservation, Cambridge University Press, Cambridge, 11–62, 2005.

Solomon, S., Dahe, Q., Martin, M., Melinda, M., Kristen, A., Melinda, M. B., T., Henry, L. M., and Zhenlin, C.: Climate Change 2007, The Physical Science Basis, Working Group I Contribution to the Fourth Assessment Report of the IPCC, Cambridge University Press, Cambridge, UK and New York, NY, USA, 2007.

Song, C., Woodcock, C. E., Seto, K. C., Lenney, M. P., and Macomber, S. A.: Classification and change detection using Landsat TM data: when and how to correct atmospheric effects?, Remote Sens. Environ., 75, 230–244, 2001.

Strahler, A. H., Woodcock, C. E., and Smith, J. A.: On the nature of models in remote sensing, Remote Sens. Environ., 20, 121–139, 1986.

Turetsky, M. R., Kotowska, A., Bubier, J., Dise, N. B., Crill, P., Hornibrook, E. R., Minkkinen, K., Moore, T. R., Myers-Smith, I. H., Nykanen, H., Olefeldt, D., Rinne, J., Saarnio, S., Shurpali, N., Tuittila, E. S., Waddington, J. M., White, J. R., Wickland, K. P., and Wilmking, M.: A synthesis of methane emissions from 71 northern, temperate, and subtropical wetlands, Glob. Change Biol., 20, 2183–2197, doi:10.1111/gcb.12580, 2014.

Usova, L.: Aerial Photography Classification of Different West Siberian Mire Landscapes, Nestor-History, Saint-Petersburg, 83 pp., 2009.
Velichko, A. A., Timireva, S. N., Kremenetski, K. V., MacDonald, G. M., and Smith, L. C.: West Siberian Plain as a late glacial desert, Quatern. Int., 237, 45–53, doi:10.1016/j.quaint.2011.01.013, 2011.
Walter, H.: The oligotrophic peatlands of Western Siberia-the largest peino-helobiome in the world, Vegetatio, 34, 167–178, 1977.
Watts, J. D., Kimball, J. S., Bartsch, A., and McDonald, K. C.: Surface water inundation in the boreal-Arctic: potential impacts on regional methane emissions, Environ. Res. Lett., 9, 075001, doi:10.1088/1748-9326/9/7/075001, 2014.
Whitcomb, J., Moghaddam, M., McDonald, K., Kellndorfer, J., and Podest, E.: Mapping vegetated wetlands of Alaska using L-band radar satellite imagery, Can. J. Remote Sens., 35, 54–72, 2009.
Xie, Y., Sha, Z., and Yu, M.: Remote sensing imagery in vegetation mapping: a review, J. Plant Ecol.-UK, 1, 9–23, 2008.





BGD
12, 20149–20178, 2015

**Table 1.** Wetland types and fractional coverage of wetland ecosystems (Water – W, Waterlogged hollows – WH, Oligotrophic hollows – OH, Ridges – R, Ryams – Ry, Fens – F, Palsa hillocks – P).

| Wetland complexes | Short description | Wetland ecosystems |
|---|---|---|
| Wooded wetlands | | |
| Pine-dwarf shrubs-sphagnum bogs (ryams) | Dwarf shrubs-sphagnum communities with pine trees (local name – "ryams") occupy the most drained parts of the wetlands. The pine height and crown density are positively correlated with the slope angle. The peat surface is usually approximately several decimeters high above the WTL. Ryams are typical oligotrophic mires that purely depend on precipitation and the atmospheric input of nutrients. Their next evolutionary type under increased precipitation or weaker drainage is RHC. | Ry: 100 % |
| Wooded swamps | Wooded swamps develop in areas enriched by groundwater flow and can be usually found in river valleys, young river terraces and parts of the floodplains farthest from the river channels. They are extremely diverse in floristic composition and have prominent microtopography. | F: 100 % |
| Patterned wetlands | | |
| Ridge-hollow complexes (RHC) | RHC are dominant in the WS taiga zone. The configuration of ridges and hollows depend on the slope angle and hydrological conditions of the contiguous areas. RHCs with small, medium, and large hollows are usually arranged within the class. | R: 42 %<br>OH: 58 % |
| Ridge-hollow-lake complexes (RHLC) | RHLCs develop from RHCs or patterned fens under permanent water stagnation or after seasonal flooding. RHLCs are the most abundant in northern taigas and occupy poorly drained watersheds. They may include the presence of numerous prolate shallow pools. The class incorporates two types: 1) with oligotrophic, 2) with meso- or eutrophic hollows. | R: 31 %<br>OH: 25 %<br>WH: 31 %<br>F: 13 % |
| Patterned fens | Patterned fens are widely distributed within the region. They correspond to the WS type of aapa mires. Patterned fens are composed of open fen environments that alternate with narrow ridges. Their vegetation cover commonly includes sedge-moss or sedge communities. | R: 28 %<br>F: 72 % |
| Palsa complexes | Palsa complexes are patterned bogs with the presence of palsa hillocks – frost heaves with heights of 0.5–1 m that contain permafrost. They appear in the north taiga and prevail northwards. | WH: 12 %<br>OH: 37 %<br>P: 51 % |
| Open wetlands | | |
| Open bogs | Open bogs are widespread along the periphery of wetland systems and are characterized by mosaic dwarf shrubs-sphagnum vegetation cover with sparse dwarf pine. | OH: 100 % |
| Open fens | Open fens are the integral class that encompasses all varieties of open rich and poor fens in WS taigas. They are confined to locations with higher mineral supplies along the periphery of large peatland systems or along peatland watercourses and areas with rich ground water supplies. The vegetation cover of open fens is characterized by higher productivity and includes sedges, herbs, hypnum and brown mosses. | F: 100 % |
| Water bodies | | |
| Lakes and rivers | This type consists of all water bodies larger than 2× 2 Landsat pixels, which can be directly distinguished by Landsat images. | W: 100 % |

**Table 2.** Latitudinal distribution of wetland ecosystem types.

| Wetland ecosystem types | South taiga | | Middle taiga | | North taiga | | Total area | |
|---|---|---|---|---|---|---|---|---|
| | Area, Mha | % | Area, Mha | % | Area, Mha | % | Area, Mha | % |
| Water | 0.37 | 3 | 1.66 | 9 | 3.91 | 19 | 5.94 | 11.3 |
| Waterlogged hollows | 0.50 | 4 | 1.32 | 7 | 3.40 | 16 | 5.22 | 10.0 |
| Oligotrophic hollows | 1.87 | 16 | 5.78 | 30 | 5.60 | 27 | 13.25 | 25.3 |
| Ridges | 1.70 | 14 | 3.61 | 19 | 3.37 | 16 | 8.69 | 16.6 |
| Ryams | 3.37 | 28 | 5.14 | 27 | 1.60 | 8 | 10.11 | 19.3 |
| Fens | 4.22 | 35 | 1.77 | 9 | 1.53 | 7 | 7.52 | 14.3 |
| Palsa hillocks | 0.00 | 0 | 0.00 | 0 | 1.71 | 8 | 1.71 | 3.3 |
| Total wetland area | 12.04 | | 19.27 | | 21.13 | | 52.44 | |
| Total zonal area | 42.96 | | 56.56 | | 58.46 | | 157.97 | |
| Paludification, % | 28.0 | | 34.1 | | 36.1 | | 33.2 | |

**Table 3.** Confusion matrix of West Siberian wetland map validation (additional 11 floodplain and 33 mixed class polygons classified as wetlands are not presented). Bold values denote overlap of real and estimated classes.

| Real classes<br>Estimated classes | Non-wetland | Lakes and rivers | RHLC | Ryams | RHC | Open Fens | Patterned Fens | Swamps | Palsa complexes | Open bogs | Total | UA[1], % |
|---|---|---|---|---|---|---|---|---|---|---|---|---|
| Non-wetland | **110** | | | 1 | | | | | | 2 | 113 | 97 |
| Lakes and rivers | | **94** | 3 | | | | | 1 | | | 98 | 96 |
| RHLC | 4 | 7 | **69** | 1 | 4 | | | | 2 | | 87 | 79 |
| Ryams | 3 | | 1 | **108** | 7 | | 4 | | | 7 | 130 | 83 |
| RHC | 1 | | 6 | 2 | **150** | 5 | 9 | | | 8 | 181 | 83 |
| Open Fens | | | 3 | 1 | 3 | **86** | 20 | | | 3 | 116 | 74 |
| Patterned Fens | 1 | | 4 | 1 | | 18 | **68** | | | | 92 | 74 |
| Swamps | 5 | | | | | 4 | 9 | **82** | | | 100 | 82 |
| Palsa complexes | 13 | | 1 | 2 | 1 | | | | **54** | 3 | 74 | 73 |
| Open bogs | | | | 1 | 7 | 1 | | | | **38** | 47 | 81 |
| Total | 137 | 101 | 87 | 117 | 172 | 114 | 110 | 83 | 56 | 61 | **1038** | |
| PA[2], % | 80 | 93 | 79 | 92 | 87 | 75 | 62 | 99 | 96 | 62 | | |

[1]UA – user's accuracy; [2]PA – producer's accuracy.





BGD
12, 20149–20178, 2015

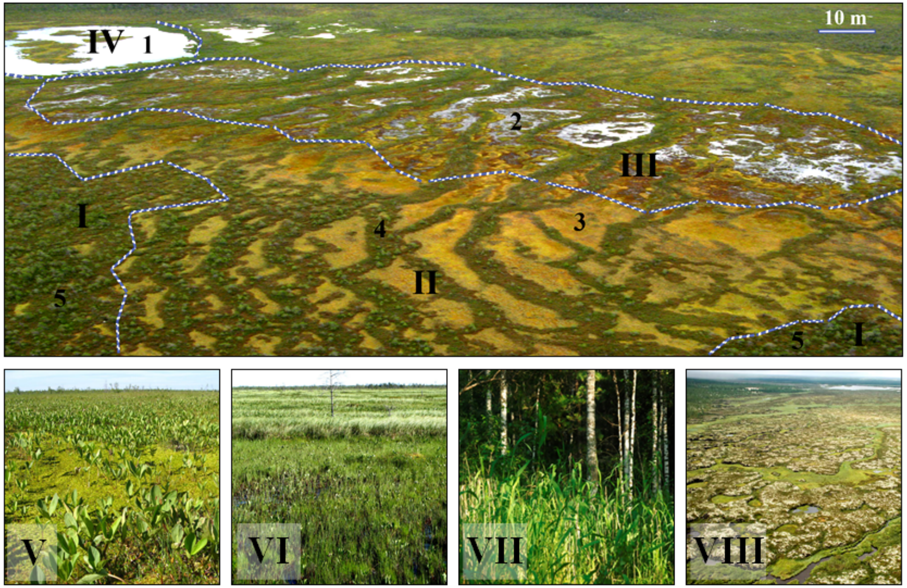


**Figure 1.** Wetland complexes (I – Ryam, II – Ridge-hollow complex or RHC, III – Ridge-hollow-lake complex or RHLC, IV – Lakes and rivers, V – Open fens, VI – Patterned fens, VII – Swamps, VIII – Palsa complexes) and ecosystems in WS (1 – Water, 2 – Waterlogged hollows, 3 – Oligotrophic hollows, 4 – Ridges, 5 – Ryams).





BGD
12, 20149–20178, 2015

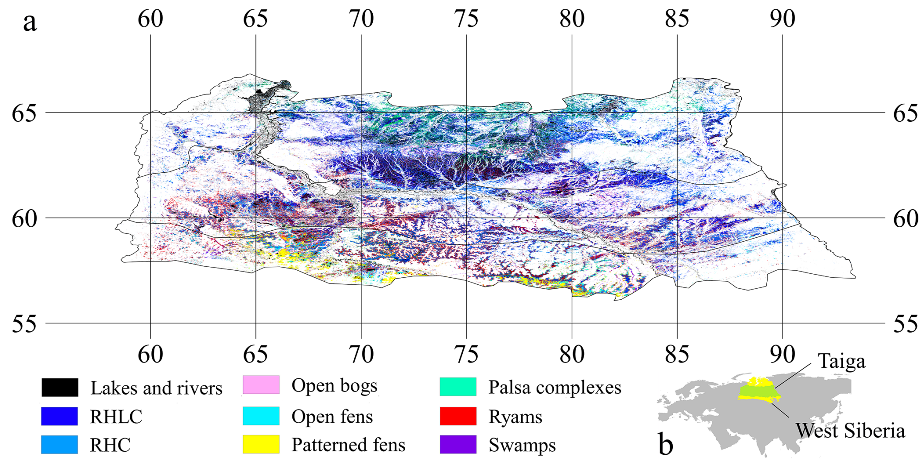


**Figure 2.** Wetland map **(a)** of the WS taiga zone (**b**; yellow – WS, green – Taiga zone).





BGD
12, 20149–20178, 2015

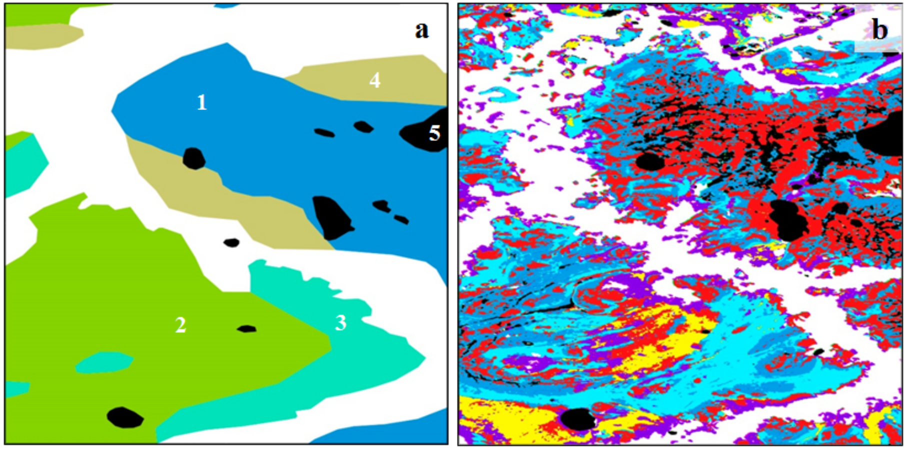


**Figure 3.** Comparison of wetland classifications: **(a)** – SHI map (1 – Sphagnum-dominated bogs with pools and open stand of trees, 2 – ridge-hollow, ridge-hollow-pool and ridge-pool patterned bogs, 3 – forested shrubs- and moss-dominated mires, 4 – moss-dominated treed mires, 5 – water bodies), **(b)** – this study (legend is on Fig. 2); 59–59.5° N, 66–66.5° E.





BGD
12, 20149–20178, 2015

High resolution wetland mapping in West Siberian taiga zone

I. E. Terentieva et al.

Title Page
Abstract | Introduction
Conclusions | References
Tables | Figures
◀◀ | ▶▶
◀ | ▶
Back | Close
Full Screen / Esc
Printer-friendly Version
Interactive Discussion

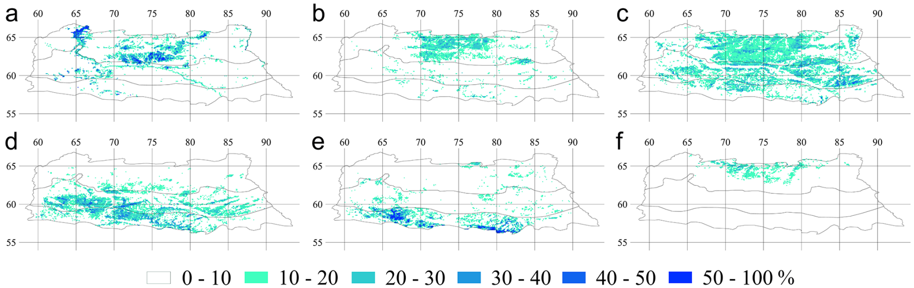


**Figure 4.** Wetland ecosystem areas for 0.1° × 0.1° (% from the total cell area): **(a)** – water, **(b)** – waterlogged hollows, **(c)** – oligotrophic hollows, **(d)** – ryams, **(e)** – fens, **(f)** – palsa hillocks; the distribution of ridges is not represented because it is quite similar to the oligotrophic hollow distribution; the black outlines divide the taiga into the north, middle and south Taiga subzones.



BGD
12, 20149–20178, 2015